2020

TDT Sandwich: An open source dry heat system for characterizing the thermal resistance of microorganisms

Soon Kiat Lau

Jeyamkondan Subbiah

HardwareX 8 (2020) e00114

Contents lists available at ScienceDirect

HardwareX

journal homepage: www.elsevier.com/locate/ohx

Hardware Article

TDT Sandwich: An open source dry heat system for characterizing the thermal resistance of microorganisms

Soon Kiat Lau [a,b], Jeyamkondan Subbiah [a,b,c,*]

[a] Department of Food Science and Technology, University of Nebraska-Lincoln, Lincoln, NE, USA
[b] Department of Biological Systems Engineering, University of Nebraska-Lincoln, Lincoln, NE, USA
[c] Department of Food Science, University of Arkansas, Fayetteville, AR, USA

ARTICLE INFO

Article history:
Received 6 February 2020
Received in revised form 3 April 2020
Accepted 4 June 2020

Keywords:
Thermal death time
Thermal death kinetics
D value
Zvalue
F value
Food safety
Low moisture foods
Isothermal
Come-up time
Uniform heating

ABSTRACT

The determination of the thermal death kinetics of microorganisms has traditionally been performed with liquid baths which have some disadvantages such as liquid spillage and liquid infiltration into samples. The TDT Sandwich was developed as a free, open source alternative that utilizes dry heat. The system is capable of heating samples up to 140 °C and maintaining it within 0.2 °C of the target temperature. Other features of the TDT Sandwich include adjustable heating rates up to approximately 100 °C/min, real-time display and recording of temperature readings at a nominal rate of 5 Hz, an optional thermocouple for acquiring temperature of samples, built-in heating timer, and customizable operating parameters. The modular nature of the TDT Sandwich allows multiple units to be connected to a computer or laptop. Operation of the TDT Sandwich is done through a computer program which, along with the build instructions and microcontroller program, are open source and are available for free to the public at https://doi.org/10.17605/OSF.IO/5Q3Y7.

Specifications Table

Hardware name	TDT Sandwich
Subject Area	• Biological Sciences • Educational Tools and Open Source Alternatives to Existing Infrastructure
Hardware type	• Measuring physical properties and in-lab sensors • Biological sample handling and preparation
Open Source License	GNU General Public License (GPL) 3.0
Cost of Hardware	173 USD per TDT Sandwich, 255 USD for 5000 consumable pouches
Source File Repository	https://doi.org/10.17605/OSF.IO/5Q3Y7

* Corresponding author at: University of Arkansas, 2650 N. Young Ave., Fayetteville, AR 72704, USA.
E-mail address: jsubbiah@uark.edu (J. Subbiah).

https://doi.org/10.1016/j.ohx.2020.e00114
2468-0672/

1. Hardware in context

A comprehensive understanding of the thermal death kinetics of pathogenic microorganisms is essential for designing and validating thermal pasteurization or sterilization technologies. By modeling the inactivation of microorganisms during a thermal treatment, the thermal death time (TDT) of the target microorganism can be calculated to characterize the robustness of the thermal treatment. The TDT is usually calculated from microbial death models containing one or more parameters that need to be determined experimentally using inoculated food samples and equipment with some form of temperature control.

In most cases, temperature-controlled liquid baths are used to control the temperature of samples in thermal death kinetics characterization studies because they are commercially available, user-friendly and suffice for most experimental needs. However, the use of liquid as a heating medium introduces the risk of water infiltration into samples which may affect results because water activity has been shown to affect the thermal resistance of bacteria in low-moisture foods [1]. There are also operational disadvantages to liquid baths such as the need to pre-heat it and cleanup of liquid spillage.

There are few custom equipment that have been developed specifically for measuring the thermal death kinetics of microorganisms. The thermoresistometer mainly consists of a vessel that has an injection port, sampling port, pressurizing port, heating coil, mixing propeller, thermocouple, and pH electrode [2–7]. Initially, bacterial inoculum is injected into preheated sterile sample in the vessel to be heated to the target temperature. Samples are then extracted at specified time intervals from the sampling port. This instrument requires proper sample preparation to ensure that they can be stirred and flow through tubes, thus it may be unsuitable for dry and granular samples. The BUGDEATH apparatus utilizes a combination of hot dry air, steam, and cold air to heat or cool the surface of a sample [8–13]. The use of the three heating/cooling systems allows reproduction of the dynamic temperature and relative humidity conditions experienced by microorganisms on the surface of a food product. However, the system is built to process only one sample at a time. The heating block system is an aluminum block padded with heating pads that has slots machined into its sides for drawers containing the samples [14–18]. Each drawer has a well in which the sample is placed and then enclosed by a screw-on cap. Although the system allows the user to adjust the heating rate, the maximum heating rate of 13.3 °C/min means that it would take a while for the sample to reach the target temperature, during which some loss of the microorganism of interest may occur. Clearly, there is no silver bullet for characterizing the thermal death kinetics of microorganisms. The introduction of additional custom equipment would provide researchers with more options to choose from to satisfy their experimental objectives.

The come-up time (CUT) of a sample can be defined as the time needed for the temperature of the sample to reach within a certain threshold of the target treatment temperature. CUT has been shown to affect the thermal resistance of bacteria and fungi in a variety of food products, with a longer CUT resulting in higher thermal resistance [10,14,17,19,20]. If researchers are provided a research tool that allows control of CUT, it will open a path for investigation into its effects on inactivation kinetics of microorganisms.

This paper describes the design, construction, operation, and performance of the TDT Sandwich which was conceived to address the limitations and needs in existing systems and to expedite the laborious process of characterizing thermal death kinetics. The build instructions and software of the TDT Sandwich are open source and available for free to allow replication of the system by other researchers.

2. Hardware description

The TDT Sandwich (Fig. 1) is a clamshell-like box that applies dry heat to a sample sandwiched between the internal heating pads. The system can raise the temperature of a sample to a desired target (up to 140 °C) and then maintain it within 0.2 °C of the target. The rate of temperature increase of the heating pads can be adjusted up to a maximum of approximately 100 °C/min. Temperature measurements are performed with type-T thermocouples with limits of error of ±0.5 °C. The electronics for the system are housed in an enclosure adhered to the top of the system that also displays the customizable identification number of the system. The TDT Sandwich connects to a computer or laptop via a USB cable and is controlled using the free software described in **Section 6.3**. Due to the wide availability of USB hubs, multiple TDT Sandwiches can be connected to a single computer or laptop and can be plugged in or out when not in operation, thus giving rise to its modular nature. Aside from the custom-order heaters and printed circuit board, the TDT Sandwich is designed to be constructed from commercially available components to simplify the construction process. A single TDT Sandwich only costs about a tenth or less of scientific programmable water baths. The system is also mess-free, maintenance-free, have few moving parts, and is easy to operate. Samples treated in the TDT Sandwich are packaged in airtight pouches which create a closed environment for the sample during heating. Because it only has heating capabilities, the TDT Sandwich is not built to cool samples rapidly. Some possible usages of the TDT Sandwich include:

- Holding a sample at a target temperature for a given period of time to measure the amount of microorganisms inactivated by the heat treatment.
- Investigating the effects of CUT on the thermal resistance of a microorganism.
- Characterizing the effects of heat on quality changes in a food sample such as lipid oxidation, color change, enzyme inactivation, and destruction of heat-labile nutrients.
- General-purpose heating of samples.

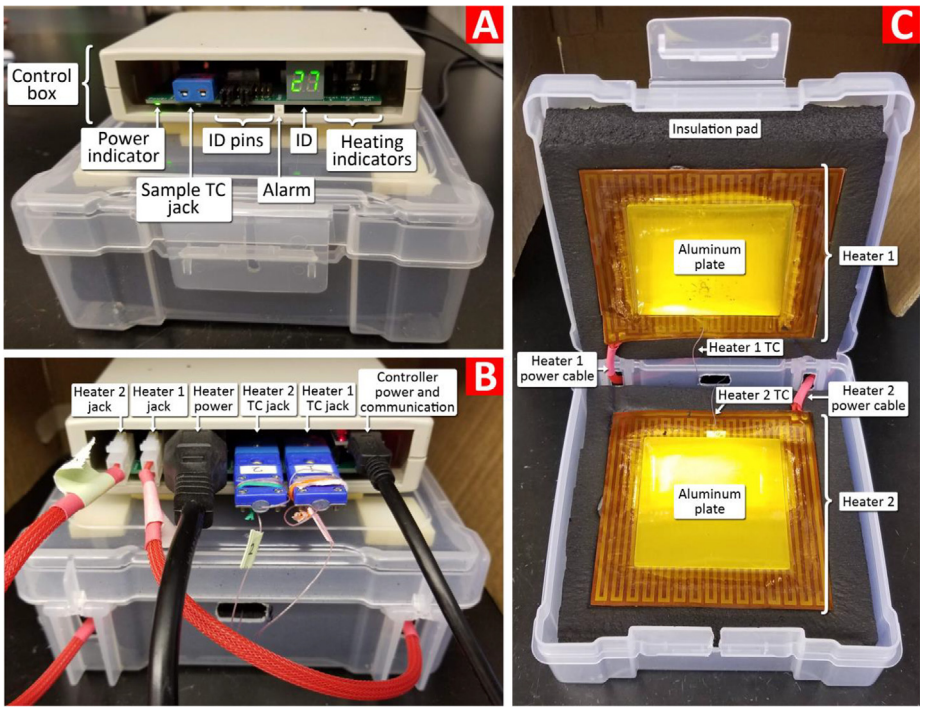

Fig. 1. Annotated views of the TDT Sandwich from the (A) front, (B) back, and (C) inside. Abbreviations used: TC = thermocouple, ID = identification.

3. Design files

All the files necessary for the construction and operation of the TDT Sandwich are listed in Table 1. The printed circuit board (PCB) design files can be sent to a PCB manufacturer to fabricate the PCB. The Arduino code is uploaded to the microcontroller of the TDT Sandwich during the construction process. The computer program is a Windows executable file for controlling TDT Sandwiches. All the files are stored in an online repository with an accompanying "Wiki" that describes the files and their uses.

4. Bill of materials

Tables 2 and 3 list all the materials needed for building a single TDT Sandwich. Some specialized tools or consumables used during the construction process are listed in Table 4. Once the TDT Sandwich has been constructed and is ready to be used, it is recommended to seal samples in the disposable pouches listed in Table 5. Decimal quantities are given for items that are sold in bulk but of which only one or a few units are needed.

5. Design and construction

This section provides instructions for constructing the TDT Sandwich and the rationale behind certain design aspects of the system.

Table 1
Design files for the TDT Sandwich.

Design file name	File type	Open source license	Location of the file
Printed circuit board design files	Electronics	GNU General Public License (GPL) 3.0	https://doi.org/10.17605/OSF.IO/WGYXP
Arduino code	Software	GNU General Public License (GPL) 3.0	https://doi.org/10.17605/OSF.IO/FE62V
Computer program	Software	GNU General Public License (GPL) 3.0	https://doi.org/10.17605/OSF.IO/EDPKU
Finite element model (unsolved)	COMSOL Multiphysics® file	GNU General Public License (GPL) 3.0	https://doi.org/10.17605/OSF.IO/5NZEP

Table 2
Bill of materials for components of the TDT Sandwich printed circuit board.

Designator	Component	Quantity	Cost per unit (USD)	Total cost (USD)	Source of materials
PCB	Printed circuit boards (Pack of 10)	0.1	$5.00	$0.50	Send PCB design files from Table 1 to a PCB manufacturer (e.g. https://jlcpcb.com/)
S1	Flat Head Screws, M2 × 0.4 mm Thread, 12 mm Long (pack of 100)	0.03	$5.60	$0.17	https://www.mcmaster.com/91420A006
S2	Hex Nut, Low-Strength, M2 × 0.4 mm Thread (pack of 100)	0.03	$1.57	$0.05	https://www.mcmaster.com/90591A111
BZ1	Buzzer, polarized	1	$1.12	$1.12	https://www.digikey.com/products/en?keywords=AI-1223-TWT-5V-5-R
C1 C3 C6 C8 C11 C13	Ceramic capacitor, 0.01 uF, 0603	6	$0.01	$0.07	https://www.arrow.com/en/products/c0603c103m5rac/kemet-corporation
C2 C4 C5 C7 C9 C10 C12 C14 C15 C16 C17 C18 C19 C20 C21 C22 C23 C24 C25 C26 C27	Ceramic capacitor, 0.1 uF, 0603	21	$0.01	$0.27	https://www.arrow.com/en/products/cl10b104ko8wpnc/samsung-electro-mechanics
D1 D2	LED, orange, R/A, 0805	2	$0.10	$0.21	https://www.arrow.com/en/products/ltst-s220kfkt/lite-on-technology
D3	LED, green, R/A, 0805	1	$0.12	$0.12	https://www.arrow.com/en/products/ltst-s220kgkt/lite-on-technology
D4	LED, red, R/A, 0805	1	$0.13	$0.13	https://www.arrow.com/en/products/ltst-s220krkt/lite-on-technology
D5	LED, amber, R/A, 0805	1	$0.61	$0.61	https://www.digikey.com/product-detail/en/osram-opto-semiconductors-inc/LA-A67F-AABB-24–1-30-R33-Z/475–3392-1-ND/7907989
F1	Fuse holder	1	$0.74	$0.74	https://www.arrow.com/en/products/64900001039/littelfuse
J8	Male headers, 16 pos, 2.54 mm pitch, R/A	1	$0.55	$0.55	https://www.arrow.com/en/products/68021-216hlf/amphenol-fci
J7	Female headers, 15 pos, 2.54 mm pitch	2	$2.20	$4.39	https://www.arrow.com/en/products/1–535541-3/te-connectivity
J1 J2 J3	Thermocouple type-T miniature connector, PCB mount	3	$3.50	$10.50	https://evosensors.com/collections/miniature-pcb-flat-mounting/products/t1x-femx-con-fp-x-pccx
J4 J5	Connector, 01x02	2	$0.21	$0.42	https://www.arrow.com/en/products/39–30-1020/molex
J6	Power entry connector, IEC320-C6	1	$1.31	$1.31	https://www.digikey.com/product-detail/en/qualtek/771W-BX2-01/Q311-ND/417925
Q1 Q2 Q3 Q4	MOSFET, N-channel, 30 V, 3.4A	4	$0.26	$1.03	https://www.arrow.com/en/products/irlml6346trpbf/infineon-technologies-ag
R1 R2 R3 R4 R5 R6	Resistor, 10 Ω, 0.1%, 0603	6	$0.09	$0.57	https://www.arrow.com/en/products/cpf0603b10re/te-connectivity
R13	Resistor, 100 Ω, 0.5 W, 1210	1	$0.09	$0.09	https://www.arrow.com/en/products/rc1210fr-07100rl/yageo
R7 R8	Resistor, 180 Ω, 0805	2	<$0.01	<$0.01	https://www.arrow.com/en/products/rmcf0805jt180r/stackpole-electronics
R21	Resistor, 1 kΩ, 0805	1	<$0.01	<$0.01	https://www.arrow.com/en/products/ac0805jr-071kl/yageo
R22	Resistor, 27 kΩ, 0805	1	<$0.01	<$0.01	https://www.arrow.com/en/products/rc0805fr-0727kl/yageo
R11 R12 R14 R15 R16 R17 R18 R19 R20 R23 R24 R25 R26	Resistor, 5.1 kΩ, 0805	13	<$0.01	$0.03	https://www.arrow.com/en/products/rc0805jr-075k1l/yageo
R9 R10	Resistor, 510 Ω, 0805	2	<$0.01	<$0.01	https://www.arrow.com/en/products/rmcf0805jt270r/stackpole-electronics
RN1	Resistor network, 8 elements, isolated, 2.2 kΩ	1	$0.17	$0.17	https://www.arrow.com/en/products/exb-2hv222jv/panasonic
RN2	Resistor network, 8 elements, isolated, 22 kΩ	1	$0.17	$0.17	https://www.arrow.com/en/products/exb-2hv223jv/panasonic
RN3	Resistor network, 8 elements, isolated, 510 Ω	1	$1.35	$1.35	https://www.arrow.com/en/products/vssr1603511guf/vishay
U4 U5	Voltage level translator, 8 bits, bidirectional	2	$0.66	$1.32	https://www.digikey.com/product-detail/en/nexperia-usa-inc/74LVC4245APW112/1727–2878-ND/763190
U6 U7	Solid state relay, zero crossing	2	$4.02	$8.04	https://www.arrow.com/en/products/cpc1966y/ixys

Table 2 (*continued*)

Designator	Component	Quantity	Cost per unit (USD)	Total cost (USD)	Source of materials
U13	LED 7-segment display, green, 10 pin, R/A	1	$2.36	$2.36	https://www.arrow.com/en/products/ldd-f302ni-ra/lumex
U1 U2 U3	Thermocouple converter	3	$4.85	$14.55	https://www.digikey.com/product-detail/en/maxim-integrated/MAX31856MUD/MAX31856MUD-ND/5050138
U9	Shift register, 8-Bit, parallel to serial	1	$0.30	$0.30	https://www.arrow.com/en/products/mc74hc589adtr2g/on-semiconductor
U8 U11 U12	Shift register, 8-Bit, serial/parallel to serial	3	$0.25	$0.75	https://www.arrow.com/en/products/74hc595pw118/nexperia
U10	CMOS timer	1	$0.32	$0.32	https://www.arrow.com/en/products/ne555pw/texas-instruments

Table 3
Bill of materials for other components of the TDT Sandwich.

Designator	Component	Quantity	Cost per unit (USD)	Total cost (USD)	Source of materials
CB1	Enclosure, ABS, gray, 5.12″L × 3.94″W	1	$4.30	$4.30	https://www.digikey.com/products/en?keywords=RM2015S
CB2	Arduino Nano V3.0 with USB cable	0.33	$12.35	$4.12	https://www.amazon.com/gp/product/B07KC9C6H5/
CB3	Fuse, 250 V, 2.5 A, fast-blow	1	$0.25	$0.25	https://www.arrow.com/en/products/021702.5mxp/littelfuse
CB4	USB-A to mini USB-B cable, 80 cm (Pack of 20)	0.05	$7.99	$0.40	https://www.ebay.com/itm/20x-5pin-Mini-B-To-A-USB-2–0-Cable-Cord-For-PC-Laptop-MP3-MP4-Digital-Camera-US/352454570522
CB5	Power cord, NEMA 5-15P to IEC 320-C15, 6 ft (Pack of 20)	0.05	$22.99	$1.15	https://www.ebay.com/itm/20-PACK-6FT-3-Prong-Mickey-Mouse-Power-Cord-Cable-for-Laptop-PC-Printer-Adapter/282413831612
CB6	Jumper, 2 positions	8	$0.32	$2.54	https://www.digikey.com/product-detail/en/880584–4/A122487-ND/1131873/?itemSeq=283547149
T1	PFA-insulated thermocouple, type T, 40″ long, 40 AWG, stripped leads	0.6	$77.90	$46.74	https://www.omega.com/en-us/wire-sensor/5tc/p/5TC-TT-T-40–36
T2	Miniature thermocouple connector, type T, male (pack of 50)	0.06	$160.43	$9.63	https://www.omega.com/pptst/SMPW-CC.html
T3	Silicone wire grommet (pack of 50)	0.06	$2.87	$0.17	https://www.omega.com/pptst/SMPW-CC.html
T4	Silicone clamp grommet (pack of 50)	0.06	$2.90	$0.17	https://www.omega.com/pptst/SMPW-CC.html
A1	Aluminum 3003 Sheet, 0.032″ Thick, 4″ × 10″ (pack of 6)	0.21	$10.25	$2.15	https://www.grainger.com/product/GRAINGER-APPROVED-Aluminum-Sheet-Stock-5MWN1
A2	Adhesive Transfer Tape, 4″ X 20 yd, 2.30 mil Thick	0.02	$66.95	$1.12	https://www.grainger.com/product/15D108
H1	Polyimide etched-foil heater, 120 mm × 120 mm, 120 V, 144 W, 1 W/cm^2, uniform etched foil pattern, no adhesive, 300 mm lead wire sealed to corner of heater with silicone	2	$15.00	$30.00	Custom-order from a manufacturer: https://jymydq.en.alibaba.com/. Contact the manufacturer and provide them with the specifications as shown on the left.
H2	Expandable Polyester Sleeving, Red, 1/8″ ID, 100′ Long	0.02	$16.01	$0.21	https://www.mcmaster.com/9284k11
H3	Heat-Shrink Tubing, Red, 25′ Long, 0.19″ ID Before Shrinking	0.02	$15.56	$0.31	https://www.mcmaster.com/7856k74
H4	Plug contacts, Female 18–24 AWG	4	$0.06	$0.25	https://www.arrow.com/en/products/39–00-0038/molex
H5	Plug, 01x02	2	$0.09	$0.18	https://www.arrow.com/en/products/39–01-2020/molex
H6	Polyimide tape, Silicone Adhesive, 4″ Wide, 15 Feet Long, 0.0025″ Overall Thickness	0.04	$45.03	$2.00	https://www.mcmaster.com/7648A717
H7	Silicone Foam Strip with Adhesive, 3/4″ Wide, 1/16″ Thick, 30′ Long	0.09	$68.48	$6.09	https://www.mcmaster.com/8645k12
B1	Polypropylene Box, 6″ × 6″ × 2″	1	$3.49	$3.49	https://www.flambeaucases.com/6-x-6-box.aspx
B2	Polyurethane Foam Mounting Tape, Open-Cell, 1/4″ Thick, 1″ Wide, 54′ Long	0.04	$87.35	$3.24	https://www.mcmaster.com/7626A132
B3	Buna-N/PVC Foam Insulation Sheet, 4′ × 36″ × 1″	0.04	$54.64	$2.28	https://www.mcmaster.com/9349K4

Table 4
Bill of materials for consumables and specialized tools used during the construction process.

Designator	Component	Quantity	Cost per unit (USD)	Total cost (USD)	Source of materials
Z1	Printed circuit board stencil	1	$13.28	$13.28	https://jlcpcb.com/
Z2	Crimping tool	1	$22.99	$22.99	https://www.amazon.com/gp/product/B00YGLKBSK/
Z3	Paper trimmer	1	$25.19	$25.19	https://www.amazon.com/gp/product/B016LDV41S/
Z4	Bastard Cut Mill File	1	$2.99	$2.99	https://www.menards.com/main/tools/hand-tools/files/tool-shop-reg-6-bastard-cut-mill-file/2446555/p-1444428087759-c-1550852385008.htm
Z5	Instant bonding adhesive, 0.5 oz	1	$4.43	$4.43	https://www.mcmaster.com/5551T72
Z6	Leaded solder paste, 63/37 No Clean, 17.6 oz	1	$59.95	$59.95	https://www.amazon.com/gp/product/B071D7SM1C/

Table 5
Bill of materials for consumables used during operation of the TDT Sandwich.

Designator	Component	Quantity	Cost per unit (USD)	Total cost (USD)	Source of materials
P1	Mylar pouches, 3″ × 3″, PAKVF4W (Case of 5000)	1	$255.00	$255.00	https://www.impakcorporation.com/flexible_packaging/mylar-bag/minipouches/03MFW03TN

5.1. Build instructions

The TDT Sandwich consists of multiple components, most of which can be constructed independently of each other before everything is assembled. Step-by-step instructions with accompanying pictures for constructing the system are provided at https://doi.org/10.17504/protocols.io.36agrae. The build instructions use the designators defined in Tables 2–4.

5.2. Design of heating system

The TDT Sandwich was built around the use of dry heat that is applied through conduction to a sample sandwiched between its two heating pads. The rationale behind this design decision is to avoid the disadvantages associated with liquid as a heating medium such as spills and contamination of samples. However, avoiding the use of liquid also means giving up its advantages such as uniform heating (when agitated) and large heatsinking capacity. Without a heatsink, the sample does not have a buffer against temperature fluctuations such as heat spikes from the heaters and heat loss to the environment. Since a uniform temperature profile is essential for ensuring the accuracy of thermal death kinetics data obtained from the TDT Sandwich, various components such as aluminum plates and insulation foam were added to the heaters in an effort to improve heating uniformity. In order to design the system for best heating performance, it would be necessary to construct multiple prototypes with varying physical configurations and run comprehensive tests on each one. To avoid this time-consuming process, a heat transfer model was developed to optimize the design of the heating system. The objective of the model was to investigate the effect of various physical configurations of the system on the heating performance. Specifically, three physical configurations were investigated: heater without aluminum plates, heater with sample-facing aluminum plate, and heater with both sample-facing and flanking aluminum plate. The model is not meant to be highly accurate and experimentally validated; instead its purpose is to provide direction for the final design of the system.

The heat conduction phenomenon in the heat transfer model is described by Fourier's law [21]:

$$\rho c_p \frac{\partial T}{\partial t} = k^2 T \tag{1}$$

where ρ is the bulk density of the material (kg m^{-3}), c_p is the specific heat capacity of the material (J kg^{-1} K^{-1}), T is the local temperature (°C), t is the current time (s), and k is the thermal conductivity of the material (W m^{-1} K^{-1}). The material properties are listed in Table 6.

As for the boundary conditions, a few characteristics of the system can be considered to simplify the model and its geometry:

- *Characteristic 1:* The heating pads are square in shape and can thus be divided into symmetrical quadrants, of which only one needs to be analyzed in the model.
- *Characteristic 2:* The two heating pads are essentially identical to each other and sandwich the sample from two opposite sides. Therefore, only one needs to be considered for the heat transfer model.

Table 6
Material properties used in the heat transfer model.

Model parameter/material property	Aluminum	Buna-N/PVC insulation foam
Density, ρ (kg m^{-3})	2700 [21]	72.08 [22]
Specific heat capacity, c_p (J kg^{-1} K^{-1})	900 [21]	1515 [23]*
Thermal conductivity, k (W m^{-1} K^{-1})	201 [21]	0.011 [22]

* No data available from manufacturer. Since the insulation material contains PVC foam, the c_p value was approximated as the average of a range of c_p values of PVC foam.

- *Characteristic 3:* Heat is generated by a resistive metal foil that forms a maze-like pattern within the heater. Due to the gaps within the maze-like pattern, heating is not strictly uniform. However, the gaps are small (2 mm) compared to the overall size of the heater (120 mm × 120 mm), therefore heating can be assumed to be uniform everywhere on the heater. The heaters are also extremely thin (0.16 mm).
- *Characteristic 4:* The insulation foam pads that flank the heaters are actually enclosed within a plastic box in the actual system. Aside from providing structural support to the TDT Sandwich, the plastic box also adds an additional layer of insulation in the form of air trapped between the walls of the box and the insulation foam pads. In this model, the worst-case-scenario is assumed where the plastic box is absent and the insulation foam pads are directly exposed to natural convection cooling by the environment.

Fig. 2 depicts the geometry, dimensions, and boundary conditions of the model based on the simplifications drawn from the characteristics of the system. Some dimensions such as thickness of the insulation foam and size of heater are fixed due to commercial availability of materials with those dimensions. To model the three investigated heater configurations, the following values as defined in Fig. 2 were used:

- Heater without aluminum plates: $l_f = l_s = d_f = d_s = 0$ cm
- Heater with sample-facing aluminum plate: l_s =4 cm, d_s = 0.08128 cm, $l_f = d_f$ =0 cm
- Heater with both sample-facing and flanking aluminum plates: $l_s = l_f$ =4 cm, $d_s = d_f$ =0.08128 cm

where l_f and l_s are one half of the side lengths of the flanking and sample-facing aluminum plates, respectively, while d_f and d_s are the thicknesses of the flanking and sample-facing aluminum plates, respectively. The above values were used due to material availability constraints (e.g. aluminum sheets are readily available in only a few thicknesses) and structural design considerations (e.g. thinner aluminum sheets deform too easily). Earlier prototypes of the TDT Sandwich also showed that a buffer zone between the edge of the heater and the edge of the sample is required to improve heating uniformity of the sample, therefore the size of the aluminum plates were adjusted to accommodate the sample while creating the aforementioned buffer zone.

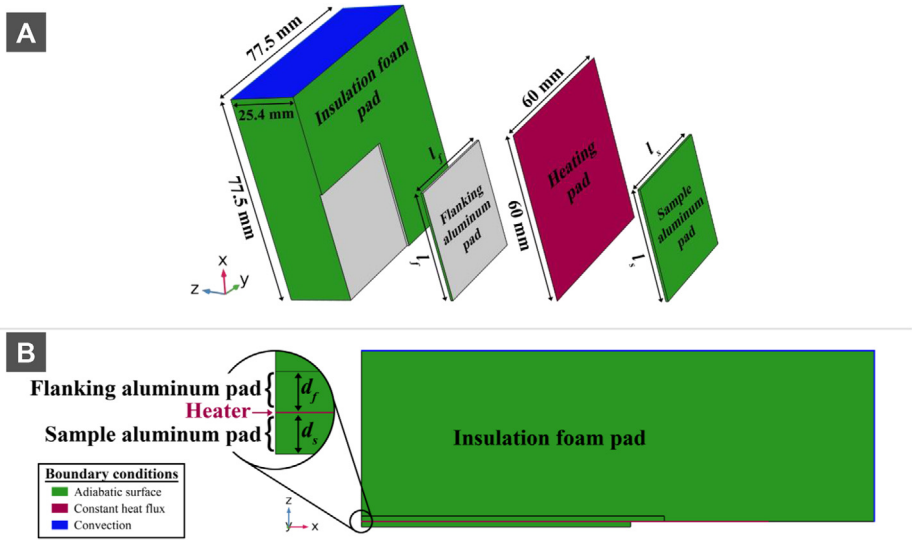

Fig. 2. Geometry, dimensions, and boundary conditions of the heat transfer model viewed from (a) an exploded diagram and (b) projection on the z-x plane.

The first and second TDT Sandwich characteristics are implemented in the geometry itself and with adiabatic boundary conditions at the symmetrical faces [21]:

$$\boldsymbol{n} \cdot \boldsymbol{q} = 0 \tag{2}$$

where $\boldsymbol{n}$ is the surface unit normal vector pointing out of the domain enclosed by the boundary and $\boldsymbol{q}$ is the heat flux at the boundary (W m^{-2}). The third characteristic implies that the heater can be modeled as a boundary heat source [21]:

$$-\boldsymbol{n} \cdot \boldsymbol{q} = Q_b \tag{3}$$

where Q_b is the boundary heat source (W m^{-2}). The negative sign implies that the heat generated by Q_b is entering the domain enclosed by the boundary. As per the assumption in the third characteristic, Q_b is assumed to be uniform over the entire heater surface. A constant temperature boundary was not used because the heater generates heat uniformly but does not guarantee a constant temperature everywhere. The value of Q_b varies during operation of the system and is modeled by a Proportional-Integral (PI) algorithm:

$$e(t) = T_{target} - T(t) \tag{4}$$

$$u(t) = K_P e(t) + K_I \int_0^t e(\tau) d\tau \tag{5}$$

$$s(t) = \begin{cases} 0, & if \quad u(t) < 0 \\ 255, & if \quad u(t) > 255 \\ u(t), & for\ other\ cases \end{cases} \tag{6}$$

$$Q_b(t) = \frac{s(t)}{255} Q_{max} \tag{7}$$

where $e(t)$ is the deviation of the process variable (in this case, temperature) from the desired target (°C), T_{target} is the desired temperature of the heater (°C), $T(t)$ is the instantaneous point temperature measured at a specific location on the heater (°C), $u(t)$ is the output of the PI algorithm, K_P is the PI proportional gain (°C^{-1}), K_I is the integral gain (°C^{-1} s^{-1}), $s(t)$ is the constrained PI output, and Q_{max} is the maximum power output of the heater (W m^{-2}). In this model and the actual TDT Sandwich system, $T_{control}$ is measured at the geometric center of the heater on the sample-facing side. The value of T_{target} was arbitrarily set to 90 °C to simulate a typical temperature used in heat inactivation studies in low-moisture foods. The values of K_p and K_i were set to 10 °C^{-1} and 0.01 °C^{-1} s^{-1}, respectively, based on some preliminary testing of the model. The PI output was not used directly as the power output of the heater; instead it was first constrained within 0 to 255 because this value range is utilized for PWM outputs in 8-bit microcontroller systems such as the Arduino Uno which is used in the TDT Sandwich system. It should be noted that the proportional term in the PI algorithm of the actual TDT Sandwich system is proportional-on-measurement instead of proportional-on-error [22], but this difference does not affect the findings of the heat transfer model.

The fourth system characteristic is modeled by convective heat flux boundary conditions on the outside-facing surfaces of the insulation foam pads [21]:

$$-\boldsymbol{n} \cdot \boldsymbol{q} = h(T_a - T_s) \tag{8}$$

where h is the convective heat transfer coefficient (W m^{-2} K^{-1}), T_a is the ambient air temperature (°C), and T_s is the temperature at the surface (°C). A value of 20 W m^{-2} K^{-1} was assumed for h to simulate natural convection without external air currents [21]. T_a was set to 25 °C to emulate room temperature conditions.

The integrated heat transfer and PI model was solved in COMSOL Multiphysics® 5.4 (COMSOL, Inc., Burlington, MA) for a 90 s heating process. The geometry was meshed with tetrahedral elements between 0.14 and 0.76 cm in size. The time-dependent problem was solved using the Multifrontal Massively Parallel Sparse (MUMPS) direct solver. The simulations were performed on a computer with a Windows 7 64-bit operating system, two Intel E5-2630 processors, and 88 GB of RAM.

Fig. 3 shows the difference between T_{target} and the temperature at the center of the surface of the sample-facing aluminum plate (or the heater, if the sample-facing plate is absent), T_{center} during the simulated heating process. Without the aluminum plates, the target temperature was quickly achieved. However, the temperature was not maintained in a stable manner and experienced some disturbance around 50 and 75 s. This behavior was unexpected because no external temperature disturbances were programmed into the model. Further refinement of the model mesh did not remove the noise. It is thus likely that these artifacts were generated from a combination of the numerical solution process and absence of a heatsink. The solution to the PI algorithm requires instantaneous integration throughout the numerical solving process and is thus prone to numerical noises. In response to these noises, the PI algorithm adjusted the output of the heater. Due to the absence of a well-conducting heatsink, the resultant spikes in heater power were not suppressed and show up in the temperature measurements. The other two configurations did not show such noises possibly due to the presence of aluminum plates as heatsinks, but the time to reach the target temperature was longer. In fact, with the addition of the flanking plate, the time was delayed by at least 50 s.

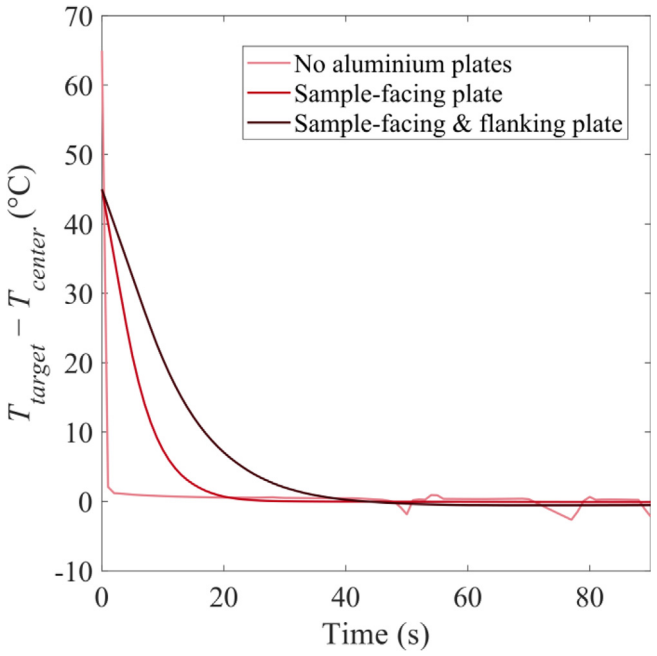

Fig. 3. Difference between the target temperature, T_{target} and the temperature at the center of the sample-facing aluminum plate (or center of the heater if the plate is absent), T_{center} during a simulated 90 s heating process for three configurations of the TDT Sandwich.

Fig. 4 plots the difference between T_{center} and the temperature at the corner of a sample pouch (**Section 5.3**), T_{corner} during the heating process. Since the pouch measures 7.62 cm by 7.62 cm, the location of T_{corner} is thus located 5.39 cm diagonally from T_{center}. During the initial heating for the heater without aluminum plates, a large difference was induced between the center and corner points. This difference was quickly minimized and stabilized at approximately 1 °C throughout the remainder of the heating process. This non-uniformity in temperature between the center and corner is undesirable. On

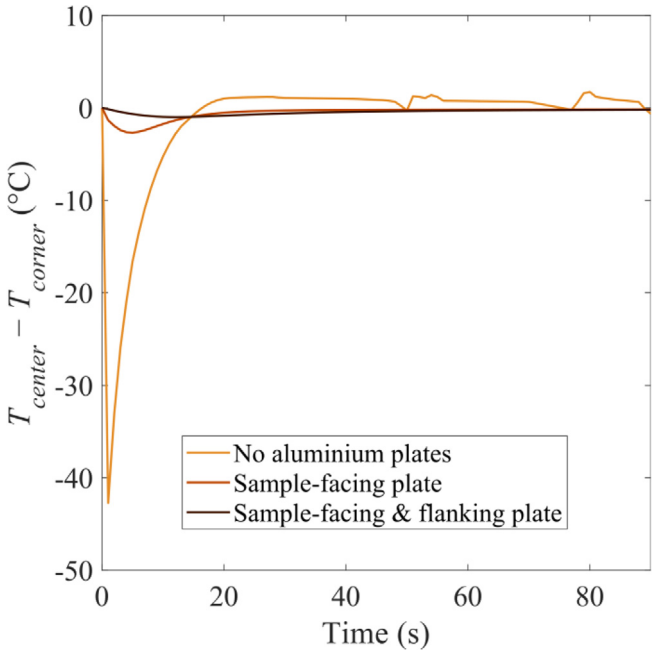

Fig. 4. Difference between the temperature at the center of the sample-facing aluminum plate (or center of the heater if the plate is absent), T_{center} and the location of the corner of an imaginary sample pouch, T_{corner} during a simulated 90 s heating process for three configurations of the TDT Sandwich.

the other hand, as aluminum plates are added onto the heater, the discrepancy in temperature between the two points is minimized. The configuration with both sample-facing and flanking aluminum plates had the best overall performance with minimal difference during the initial heating phase and the subsequent temperature maintenance phase. In addition to these simulation results, real-life tests with physical prototypes showed that the sample-facing aluminum plate on heaters without the flanking aluminum plate often peeled off during use. The addition of the flanking aluminum plate helped to mechanically secure both aluminum plates to the heater. Therefore, the configuration with both sample-facing and flanking aluminum both was used in the final design of the TDT Sandwich. Although this resulted in a prolonged initial heating phase, the improved structural integrity and heating uniformity makes this configuration the desirable choice for the design objectives of the TDT Sandwich. The temperature contour plots (Fig. 5) of this configuration over the duration of the heating process shows that the largest difference in temperature on the sample-facing aluminum plate will always be between the center and corner. This observation can be used to evaluate the heating uniformity of the physical prototypes of TDT Sandwich by placing one thermocouple at the center and another at a corner.

5.3. Choice of sample pouch

A thermal death kinetic study usually requires sealing the food sample in a sterile vessel to prevent contamination of the sample during the heating process. Various vessels for liquid and granular products have been used: test tubes [19,20,23,24], thin capillary tubes [25–29], and miniature vials such as PCR tubes [30,31]. For irregular solids or viscous samples, it may be desirable to use vacuum or heat-sealed pouches [32–38] to ensure that the vessel conforms to the shape of the sample. Alternatively, reusable vessels such as the TDT disk could be used [33,39–43]. In some cases, the food itself (e.g. shell eggs) is the vessel [44]. The choice of vessel is important to ensure excellent heat transfer during heating while minimizing the risk of contamination of the sample. Since the TDT Sandwich was constructed to apply dry heat over a large flat surface, flat pouches (03MFW03TN, IMPAK Corp., Los Angeles, CA) were used as the sample vessels. These heat-sealable pouches measure 7.62 cm $\times$ 7.62 cm and are made of thin (0.1143 mm) Mylar film metallized with aluminum, thus giving it very low diffusion properties for water vapor (1.94×10^{-4} g $m^{-2}h^{-1}$). As a result, samples can be sealed in the pouches in advance of experiments and can be used for experiments over multiple days without significant changes to the water activity of the sample. The flexibility of the pouches makes it suitable for food products in the form of liquid, paste, or powder. As these pouches are meant to contain food samples, they can be used immediately without pre-sterilization. It should be noted that the impermeability of the pouches preserves moisture content of the sample during heating, thus simulating a food product sealed in an airtight container undergoing a heating process.

Since the pouches would be subjected to high temperatures which could change the moisture permeability of the pouches, a study was performed to investigate the moisture loss from samples at elevated temperatures. Seven pouches were filled with 2.0 ± 0.1(SD) g of deionized water, sealed with a heat sealer (IPK-105H, IMPAK Corporation, Los Angeles, CA) set to level 6.5, and heated to 100 °C for a total heating time of 45 min. After the heating process, the pouches were cooled to room temperature in a desiccator before being weighed to determine the mass change. There was minimal loss in moisture (0.20 ± 0.12(SD) mg), therefore the pouches can be considered impermeable to moisture migration during isothermal treatments.

When using the pouches for thermal inactivation studies, it is advisable to ensure that the contents of the pouches are distributed evenly to improve heating uniformity. This is especially important for powder samples which tend to settle towards one edge of the pouch. To distribute the sample evenly, simply hold the pouch on the edge where most of the sample has settled on and flick it up and down. This helps to distribute the sample away from the edge. Subsequently, shake the pouch horizontally to encourage uniform distribution of the sample. As for liquid or paste samples, the distribution of the sample can be improved by simply pinching parts of the pouch which seems to have more sample than other parts of the pouch. At the conclusion of the thermal treatment, the sample can be cooled very quickly by removing them from the TDT Sandwich and submerging them into an ice slurry bath. The author and other early users of the TDT Sandwich have

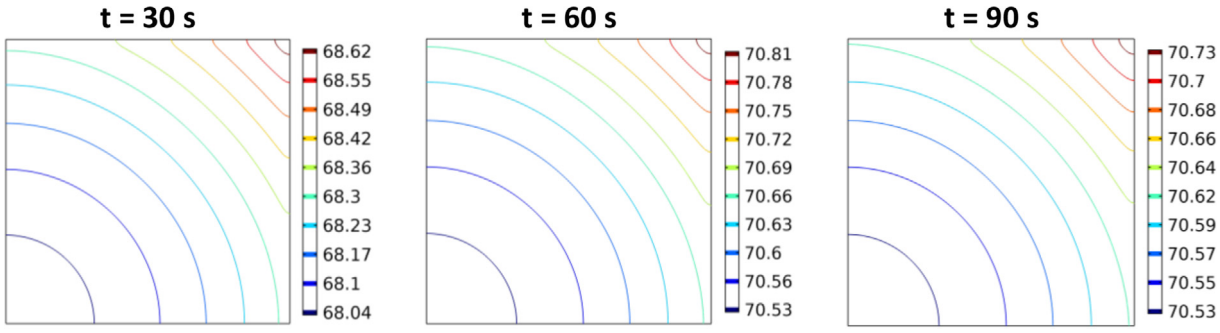

Fig. 5. Temperature contour plots on a quadrant of the sample-facing aluminum plate at select timepoints during a simulated 90 s heating process for a TDT Sandwich configured for heaters with both sample-facing and flanking aluminum plates.

performed this transfer with typical thin disposable nitrile gloves on samples up to 90 °C without issues due to the low thermal mass of the pouch, though a pair of tongs could be used if the sample is too hot to the touch.

5.4. Proportional-Integral algorithm

The heater output from the system in response to temperature readings from both heating pads are determined by a Proportional-Integral (PI) algorithm. As previously described in **Section 5.2**, the PI algorithm consists of a proportional and integral term. The proportional term responds to the immediate deviation of the process variable from the target while the integral term keeps track of the deviation over time. The TDT Sandwich uses a modified PI algorithm, whereby the proportional term is defined as proportional-on-measurement instead of proportional-on-error. With this change, the proportional term resists changes in the process variable to provide a slightly sluggish performance in exchange for improved stability and less overshoot [22]. In addition, the system was better at maintaining the temperature of the sample at the target temperature if the proportional and integral gains were forced to certain values when the heating pad temperatures were close to the target temperature. As such, the resulting PI algorithm is as follows:

$$e_P(t) = T(t) - T(t=0) \tag{9}$$

$$e_I(t) = T_{target} - T(t) \tag{10}$$

$$u(t) = -K_P e_P(t) + K_I \int_0^t e_I(\tau) d\tau \tag{11}$$

$$K_P = \begin{cases} K_{P,U}, & if \quad e_I(t) > T_P \\ K_{P,C}, & otherwise \end{cases} \tag{12}$$

$$K_I = \begin{cases} K_{I,U}, & if \quad e_I(t) > T_I \\ K_{I,C}, & otherwise \end{cases} \tag{13}$$

where $e_P(t)$ is the proportional error term (°C), $T(t)$ is the instantaneous temperature of the heating pad (°C), $T(t=0)$ is the temperature of the heating pad at the start of the heating (°C), $e_I(t)$ is the integral error term (°C), T_{target} is the target temperature for the heating pads (°C), $u(t)$ is the output of the PI algorithm, K_P is the proportional gain ($°C^{-1}$), K_I is the integral gain ($°C^{-1\text{-}s}$), $K_{P,U}$ is the user-defined proportional gain during initial heating ($°C^{-1}$), and $K_{P,C}$ is the constant proportional gain that is used when $e_I(t)$ is within the threshold T_P. $K_{I,U}$, $K_{I,C}$, and T_I are similar to their proportional counterparts, but are defined for the integral term. The values of $K_{P,U}$ and $K_{I,U}$ can be modified by the user using the computer program described in **Section 6.3**, with default values of 25.0 and 1.7, respectively. $K_{P,C}$, T_P, $K_{I,C}$, and T_I are constant values hard-coded as 5.0, 0.0, 0.8, and 0.3, respectively, into the microcontroller program of the TDT Sandwich. These values were determined through trial-and-error and should not be modified unless the user wishes to adapt the TDT Sandwich to special use cases.

6. Operation instructions

This section describes the steps for using the TDT Sandwich to heat a sample. The designators listed in Tables 2–5 will be used to describe some components for brevity.

6.1. ID of TDT Sandwich

Before using a TDT Sandwich, its identification number (ID) should first be set. Every TDT Sandwich must have a unique ID; if two or more TDT Sandwiches share the same ID, only one of them would work properly. Before setting the ID, ensure that the TDT Sandwich is not turned on *i.e.* CB4 and CB5 are disconnected. To set the ID, an appropriate amount of CB6 must be placed on certain pins at the front of the control box. By referring to the labelled pins in Fig. 6**(A)**, the following equation can be used to determine which pins CB6 should be attached to:

$$n = \sum_{i=0}^{7} a_i 2^i \tag{14}$$

where n is the ID of the TDT Sandwich, i is the pin number as labelled in Fig. 6**(A)** and on the control box, and a_i is 1 if CB6 is attached to pin i and 0 otherwise. Internally, the ID is capped to a maximum of 99. The setting of ID with the pins actually follows a binary system. Therefore, the following steps can be used to determine which pins should be plugged with C6:

1. Determine the desired ID of the TDT Sandwich and denote this as m.
2. Determine the largest value of i where 2^i is still smaller or equal to m. Denote this value of i as k.

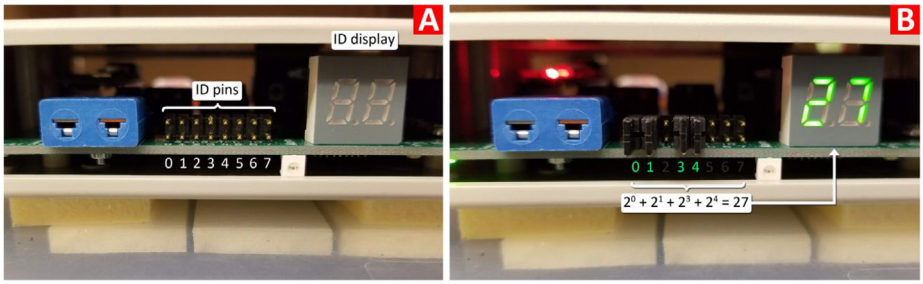

Fig. 6. Pictorial guide for setting the ID of a TDT Sandwich: (A) The pins and display for the ID; (B) An example pin configuration for a sandwich with ID 27.

3. Plug a C6 into pin k.
4. Calculate $p = m - 2^k$. If p is zero, no further action is necessary. Otherwise, repeat steps 2 to 4 by replacing m with p.

For example, for an ID of 27, pins 4, 3, 1, and 0 will be plugged with C6 (Fig. 6**(B)**). When attaching C6 to the pins, it actually connects two pins vertically. Do not connect the pins horizontally. Subsequently, ensure that the TDT Sandwich is connected to an electrical outlet or power strip with CB5 and to a computer/laptop either directly or through a USB hub with CB4. When the computer/laptop or USB hub is switched on, there will be an approximately 5 s delay before the ID of the TDT Sandwich is displayed on the display at the front of the control box. If this number is not the correct ID, refer again to the steps above to set the correct ID.

6.2. Sample preparation

If the TDT Sandwich is being used to heat a sample, it is recommended to package the sample in the pouches (P1) suggested in Table 5 and **Section 5.3**. If an exact amount of sample is needed, then the filling process should be done on a weighing scale. Otherwise, kitchen measuring spoons of an appropriate volume can be used to fill the pouches with samples. Once a pouch has been filled, its opening should be sealed with a heat sealer. For some experiments such as measuring the time taken for the sample to reach the target temperature, it is desirable to have a thermocouple in the pouch to measure the temperature of the sample during heating. To insert the thermocouple, puncture one end of the pouch with a thin sharp object such as a push pin and insert the thermocouple to a desired location in the pouch. It is recommended to place a piece of tape on the hole on the pouch to immobilize the thermocouple and minimize sample leakage (Fig. 7**(A)**).

Once the sample pouch is ready, it should be placed at the geometric center of the bottom heating pad of the TDT Sandwich (Fig. 7**(B)**). If a thermocouple is inserted into the sample, it should be routed out through the slot hole at the front of the TDT Sandwich. Subsequently, the top half of the TDT Sandwich should be secured to the bottom half by applying downwards pressure on the top half and pushing in the plastic clip at the front (Fig. 7**(C)**). The plastic clip will make a snapping or clicking sound when pushed in properly. If a thermocouple was inserted into the sample, connect the thermocouple connector to the thermocouple jack at the front of the control box (Fig. 7**(D)**). The TDT Sandwich is now ready for operation using the computer program. Note that in most use cases, the sample thermocouple is unnecessary, therefore the preparation of the TDT Sandwich is as simple as placing the pouch containing sample at the geometric center of the bottom heating pad and snapping the TDT Sandwich close.

6.3. Computer program

Instructions on downloading and installing any required files for the computer program are given in the build instructions described in **Section 5.1**. Throughout this section, elements in the program will be referred to using the labels in Fig. 8.

6.3.1. Overview

The physical TDT Sandwiches cannot be operated on their own and can only be controlled with the provided computer program. Before opening the computer program, all the TDT Sandwiches that will be used should first be connected to the computer/laptop, either directly or through USB hubs. Also, ensure that the ID for each TDT Sandwich is unique.

The computer program is a graphical user interface that contains buttons and text boxes for user input (Fig. 8). The menu bar at the top contains two items (**C0** and **P0**) that will expand to more items when they are clicked. The main body of the program lists "virtual" TDT Sandwiches. A virtual TDT Sandwich is a collection of temperature readings, heating settings, data recording functions, and various instructions to communicate with a physical TDT Sandwich. There is no limit to the amount of virtual TDT Sandwiches that can be added. In order to match a virtual TDT Sandwich to its virtual counterpart, the appropriate communication port must be assigned to it, as will be described in **Section 6.3.2**. If any errors are encountered during operation of the TDT Sandwich program, the details of the errors will be recorded in a file named "errorLog.txt" in the same directory as the TDT Sandwich program.

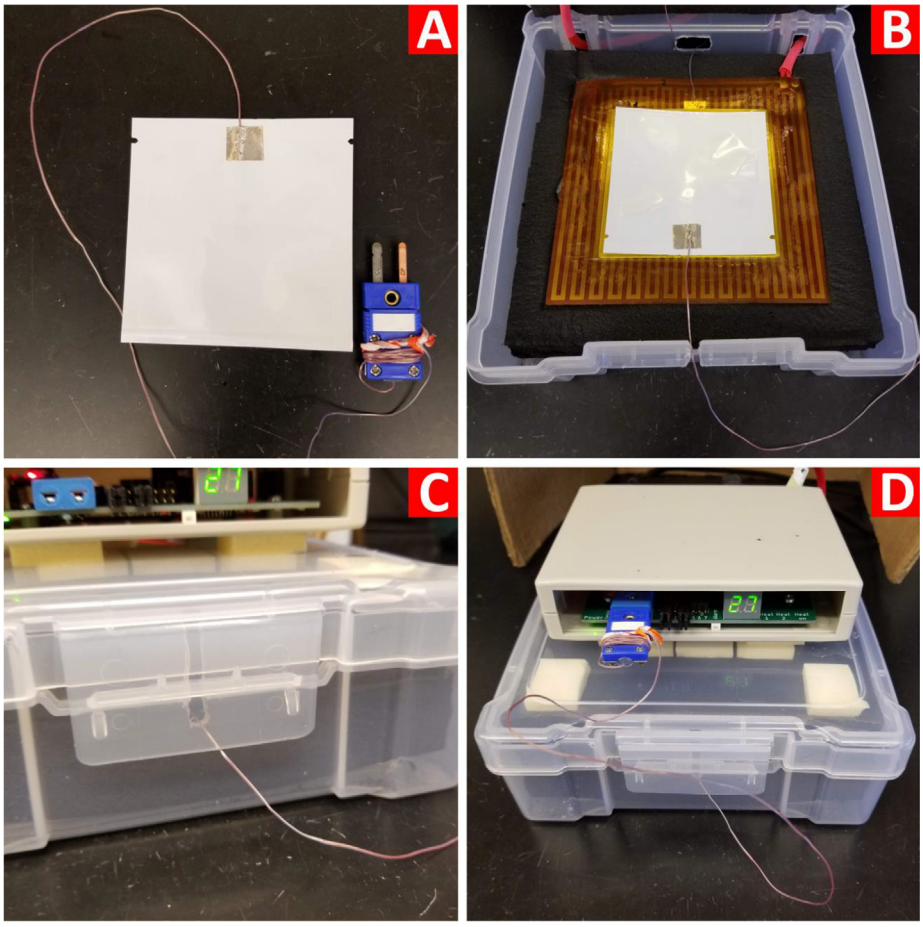

Fig. 7. Preparation of a TDT Sandwich for operation: (A) Packing sample into a pouch, sealing, and (optional) inserting a thermocouple, (B) placing the packed sample on the bottom heating pad and (optional) routing the sample thermocouple out through the front slot hole, (C) Snapping the front clip shut, and (D, optional) plugging the sample thermocouple plug into the jack at the front of the control box.

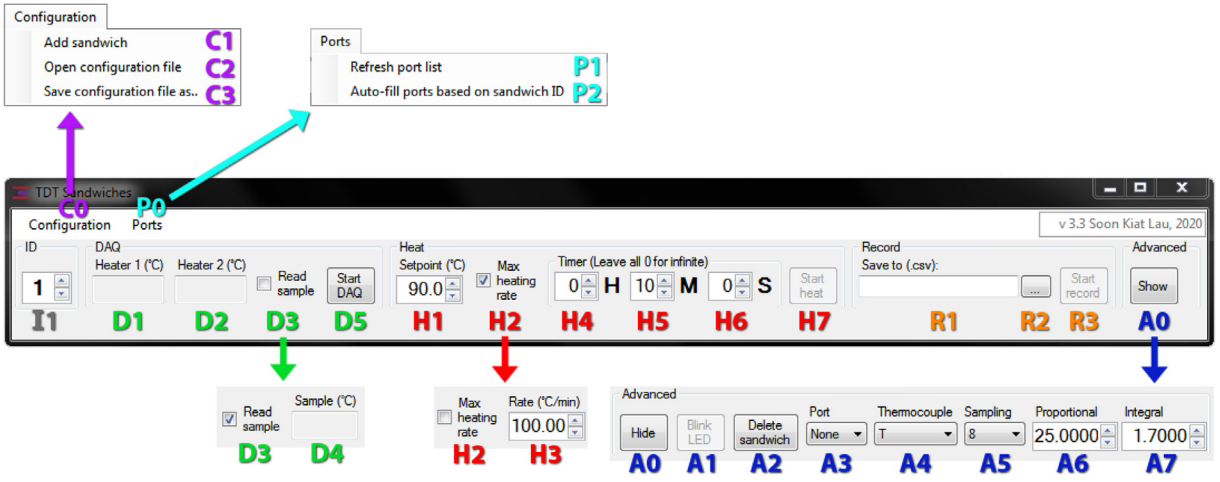

Fig. 8. Annotated view of the TDT Sandwich computer program, with expanded menus, for a single virtual TDT Sandwich. The labels are used in the text.

6.3.2. Basic operation of TDT Sandwich

Pressing **C0** and then **C1** in the program window creates a virtual TDT Sandwich that would appear below the list of existing virtual TDT Sandwiches. The default ID (**I1**) of new virtual TDT Sandwiches is 0, which should be changed to match the physical TDT Sandwich by pressing the up or down arrows on **I1** to set the ID between 0 and 99. The user can add as many virtual TDT Sandwiches to match the number of physical TDT Sandwiches. For the program to communicate with the physical TDT Sandwich, the appropriate communication port must be given (**A3**). Instead of doing this manually, it is highly recommended to press **P0** and then **P1**, before pressing **P0** again and then **P2**. **P1** instructs the program to rebuild its list of active USB connections while **P2** sends out messages to each USB port to identify if the connected device is a TDT Sandwich, obtain the ID of the connected TDT Sandwich, and populates **A3** with the appropriate communication port.

Once the virtual TDT Sandwiches have been matched to their physical counterparts, operation of the TDT Sandwiches can begin. If a thermocouple is inserted into the thermocouple jack in the front (*i.e.* the sample thermocouple), ensure that **D3** is checked so that the program would obtain and display the temperature readings of the sample (**D4**). Otherwise, keep **D3** unchecked to hide **D4**. Pressing **D5** will begin communication with the physical TDT Sandwich and acquisition of temperature readings from both heaters (**D1** and **D2**) and, if requested, the sample (**D4**). The background of the "DAQ" section will also change to green. If the incorrect communication port was selected, an error would pop up and the user should assign the appropriate port, either manually or automatically as described previously. If "Error" is displayed in either **D1**, **D2**, or **D3**, the thermocouple connection is compromised. This could be something simple like a loose connection or a serious issue like a broken thermocouple. If it was the former, the affected thermocouple should be unplugged, checked for any knots or kinks in its wire, then plugged back in. The latter requires repair or replacement of the broken thermocouple. The rate of data acquisition is affected by the number of thermocouple readings averaged (**A5**). At a default value of 8, the data acquisition rate is approximately 5 Hz. While data acquisition is active, **D5** can be pressed to stop data acquisition.

Once data acquisition has begun, the heating and recording options will be unlocked. The target temperature for the TDT Sandwich can be adjusted at **H1**, with a minimum value of 0 °C and maximum value of 140 °C. Note that this is the target temperature for the heating pads; in normal use cases, the sample temperature will eventually reach this value. However, for extremely thick samples, the isothermal sample temperature may have an offset from the heating pad temperature; this needs to be verified using the sample thermocouple. By default, **H2** is checked to induce the maximum heating rate; unchecking it reveals an input (**H3**) for adjusting the heating rate for the TDT Sandwich between 0 and 100 °C/min. The TDT Sandwich will attempt to match the given heating rate but there will be some deviation during the start of heating and close to the target temperature due to efforts by the PI algorithm to prevent the heating pad temperature from overshooting the target temperature. For most use cases where it is desirable to heat the sample as fast as possible, it is recommended to leave **H2** checked. The duration for the heating can be adjusted with **H4**, **H5**, and **H6**. The maximum duration possible is 99 h, 59 min, and 59 s. Upon pressing **H7**, the TDT Sandwich will begin applying heat according to the given settings and changes the background of the "Heat" section to red. When the remaining heating duration is 10 s or less, the TDT Sandwich will beep and flash once every second until the heating is completed, upon which it will give out an extended beep and flash. While heating is active, **H7** can be pressed to stop the heating.

The recording section allows the user to record temperature readings from the TDT Sandwich into a file. **R2** opens a window for browsing to the location to save the recorded data and giving the name for the data file. The data file is a Comma Separated Value (CSV) file which can be opened by any text processing or spreadsheet software such as Microsoft Excel. Once the location of the file has been chosen, its path will appear in **R1**. Pressing **R3** anytime while data acquisition is active, whether heating is active or not, will begin recording data to the file at the same rate that data is being acquired and changes the background of the "Record" section to yellow. Data is written into the file as new rows for each acquired data, with the first column being time (ms), second being temperature of heating pad 1 (°C), third being temperature of heating pad 2 (°C), and, if **D3** was checked, the fourth being temperature of the sample (°C). Fresh data is always appended to the end of the file; this means that if the user accidentally recorded data to an existing data file, the old contents will not be overwritten and the new data will be below the old data.

6.3.3. Configuration files

After adding a desired amount of TDT Sandwiches and adjusting their operating parameters, it may be desirable to save the program state (*i.e.* number of virtual TDT Sandwiches, heating rate, target temperature, data record location, etc.) so that it can be reused in the future instead of manually redoing the entire process. The computer program implements this feature through the use of configuration files. To save the program state at any given time, press **C0** and then **C3**. A window would open in which the user should choose a location and file name to store the program state. To load the program state, press **C0**, then **C2** and browse to the desired configuration file. The program will inform the user that the current program state will be cleared before loading the program state defined in the configuration file.

Another method of using the configuration file is to have it loaded automatically upon opening the program. When opening the computer program, the program will search for a file named "defaultConfig.csv" in the same directory as the program. If this file exists, the program will load the program state defined in that file it just like any other configuration file. This feature is useful when a known number of TDT Sandwiches with a set of default settings is to be used frequently. To use this feature, simply rename a desired configuration file to "defaultConfig.csv" without the quotes and place it in the same directory as the computer program.

6.3.4. Advanced options

The steps described in **Section 6.3.2** would suffice for most use cases of the TDT Sandwich. However, if desired, there are more options available to modify behavior of the TDT Sandwich to the user's needs. These advanced options are revealed by pressing **A0**. **A1** instructs the physical TDT Sandwich to flash for a few seconds. This is useful for checking if the correct communication port has been selected in **A3** or for finding the physical TDT Sandwich**.** Clicking **A2** removes the virtual TDT Sandwich from the list. **A3** is used to manually assign the communication port of the TDT Sandwich. **A4** and **A5** are settings affecting all the thermocouples, including the sample thermocouple. **A4** allows the user to choose a thermocouple of different type. Note that the bills of materials and build instructions utilize thermocouples of type T, so this setting should not be changed in most use cases. **A5** adjusts the number of raw thermocouple readings that are averaged to produce a final thermocouple reading *i.e.* the one that is displayed in the computer program and recorded. A smaller value increases data acquisition rate but reduces the precision of the acquired temperature reading. The default value of 8 results in a data acquisition rate of approximately 5 Hz. The proportional and integral gains of the PI algorithm in the TDT Sandwich can be adjusted with **A6** and **A7**. The default values of 25.0 and 1.7 for **A6** and **A7**, respectively, were determined through trial-and-error and provide satisfactory heating speed and temperature maintenance. If desired, the user can adjust these settings to further optimize heating performance of the TDT Sandwich.

7. Validation and characterization

The primary goal of the TDT Sandwich is to utilize dry heat to maintain a uniform temperature throughout the sample after achieving a desired CUT. However, innate variations due to manufacturing defects or human error during fabrication may affect the performance consistency among different TDT Sandwich units. It is thus necessary to verify that the system can consistently achieve its design goals under a variety of operating conditions, namely heating pad target temperature, heating pad heating rate, and sample amount.

The characterization study was performed with three heating pad target temperatures (70, 90, 110 °C), three heating pad heating rates (25, 50, ~100 °C/min) and three amounts of whole milk powder for the sample (0, 2, 4 g). To induce the maximum heating rate, the TDT Sandwiches were instructed to heat samples at 600 °C/min instead of exactly 100 °C/min in order to push the systems to their limits; the actual conservative maximum heating rate is approximately 100 °C/min. The samples masses of 2 and 4 g resulted in sample thicknesses of 1.10 ± 0.15(SD) mm and 2.00 ± 0.23(SD) mm, respectively. The experimental unit is a TDT Sandwich unit—12 units were used for this study. The consistency and innate variations of the TDT Sandwich units were measured by four characteristics:

Table 7
Characteristics of the TDT Sandwich system measured with 12 TDT Sandwich units. Values are displayed as mean (standard deviation). The reader is referred to the text for explanation of the symbols.

Sample amount (g)	Target temperature (°C)	Heating rate (°C/min)	t_{CUT}(s)	$T_u^{t_{CUT}}$(°C)	$T_u^{t_{SS}}$(°C)	$T_o^{t_{SS}}$(°C)
0	70	25	138.6 (2.6)	−0.27 (0.15)	−0.17 (0.11)	0.00 (0.10)
		50	93.9 (2.8)	−0.30 (0.10)	−0.15 (0.08)	−0.02 (0.15)
		max	57.8 (4.5)	−0.4 (0.16)	−0.19 (0.08)	0.06 (0.12)
	90	25	187.4 (1.8)	−0.32 (0.19)	−0.20 (0.10)	0.03 (0.1)
		50	117.3 (3.2)	−0.42 (0.17)	−0.17 (0.09)	0.07 (0.09)
		max	61.8 (3.5)	−0.57 (0.22)	−0.23 (0.09)	0.03 (0.1)
	110	25	232.6 (1.8)	−0.33 (0.14)	−0.19 (0.11)	0.00 (0.09)
		50	140.7 (1.9)	−0.47 (0.12)	−0.23 (0.09)	0.06 (0.09)
		max	70.0 (5.1)	−0.71 (0.35)	−0.32 (0.10)	0.08 (0.16)
2	70	25	139.8 (2.4)	−0.27 (0.14)	−0.13 (0.12)	0.04 (0.22)
		50	93.6 (1.9)	−0.27 (0.19)	−0.17 (0.12)	−0.01 (0.07)
		max	55.1 (5.4)	−0.37 (0.23)	−0.18 (0.15)	0.01 (0.11)
	90	25	189.4 (4.0)	−0.38 (0.19)	−0.17 (0.14)	0.05 (0.13)
		50	118.1 (1.6)	−0.51 (0.20)	−0.23 (0.11)	0.05 (0.10)
		max	59.3 (4.9)	−0.63 (0.45)	−0.23 (0.12)	0.13 (0.13)
	110	25	237.1 (2.1)	−0.38 (0.18)	−0.19 (0.12)	0.00 (0.07)
		50	141.3 (2.5)	−0.50 (0.23)	−0.23 (0.12)	−0.01 (0.10)
		max	68.0 (2.4)	−0.96 (0.52)	−0.32 (0.15)	0.21 (0.23)
4	70	25	141.8 (2.4)	−0.45 (0.18)	−0.19 (0.13)	0.01 (0.14)
		50	96.9 (2.7)	−0.49 (0.15)	−0.17 (0.12)	−0.02 (0.10)
		max	52.9 (6.5)	−0.84 (0.48)	−0.21 (0.16)	0.30 (0.39)
	90	25	190.1 (2.7)	−0.53 (0.17)	−0.23 (0.13)	−0.02 (0.08)
		50	122.3 (2.6)	−0.66 (0.16)	−0.23 (0.16)	0.05 (0.17)
		max	66.7 (6.8)	−1.33 (0.43)	−0.32 (0.14)	0.48 (0.34)
	110	25	238.6 (2.8)	−0.62 (0.17)	−0.20 (0.13)	−0.01 (0.07)
		50	145.1 (2.2)	−0.78 (0.21)	−0.32 (0.14)	0.02 (0.09)
		max	73.9 (3.1)	−1.63 (0.54)	−0.30 (0.17)	0.88 (0.44)

- t_{CUT} : The time (s) taken by the center of the sample to reach within 0.5 °C of the target temperature of the heating pads. Small variations in CUT for a set of TDT Sandwich units indicate minimal variation between the TDT Sandwich units.
- $T_u^{t_{CUT}} = T_{center}^{t_{CUT}} - T_{corner}^{t_{CUT}}$: The difference in temperature (°C) between the center and corner of the sample at the time when CUT was achieved. The smaller the difference, the more uniform the heating of the sample. If this number is negative, then the center of the sample is colder than the corner. The temperature measurement locations were chosen based on the heat transfer model in **Section 5.2** which predicted the largest temperature difference between the center and corner.
- $T_u^{t_{SS}} = T_{center}^{t_{SS}} - T_{corner}^{t_{SS}}$: Same as $T_U^{t_{CUT}}$, but 1 min after achieving CUT *i.e.* $t_{SS} = t_{CUT} + 1$ min. The time delay of 1 min was arbitrarily chosen to capture steady-state (SS) condition of the heating pad and sample within a reasonable time frame.
- $T_o^{t_{SS}} = T_{center}^{t_{SS}} - T_{target}^{t_{SS}}$: The difference between the temperature at the center of the sample and the target temperature of the heating pad 1 min after achieving CUT. A minimal value is desired so that the user does not have to apply offsets to the target temperature of the heating pad to achieve a desired sample temperature.

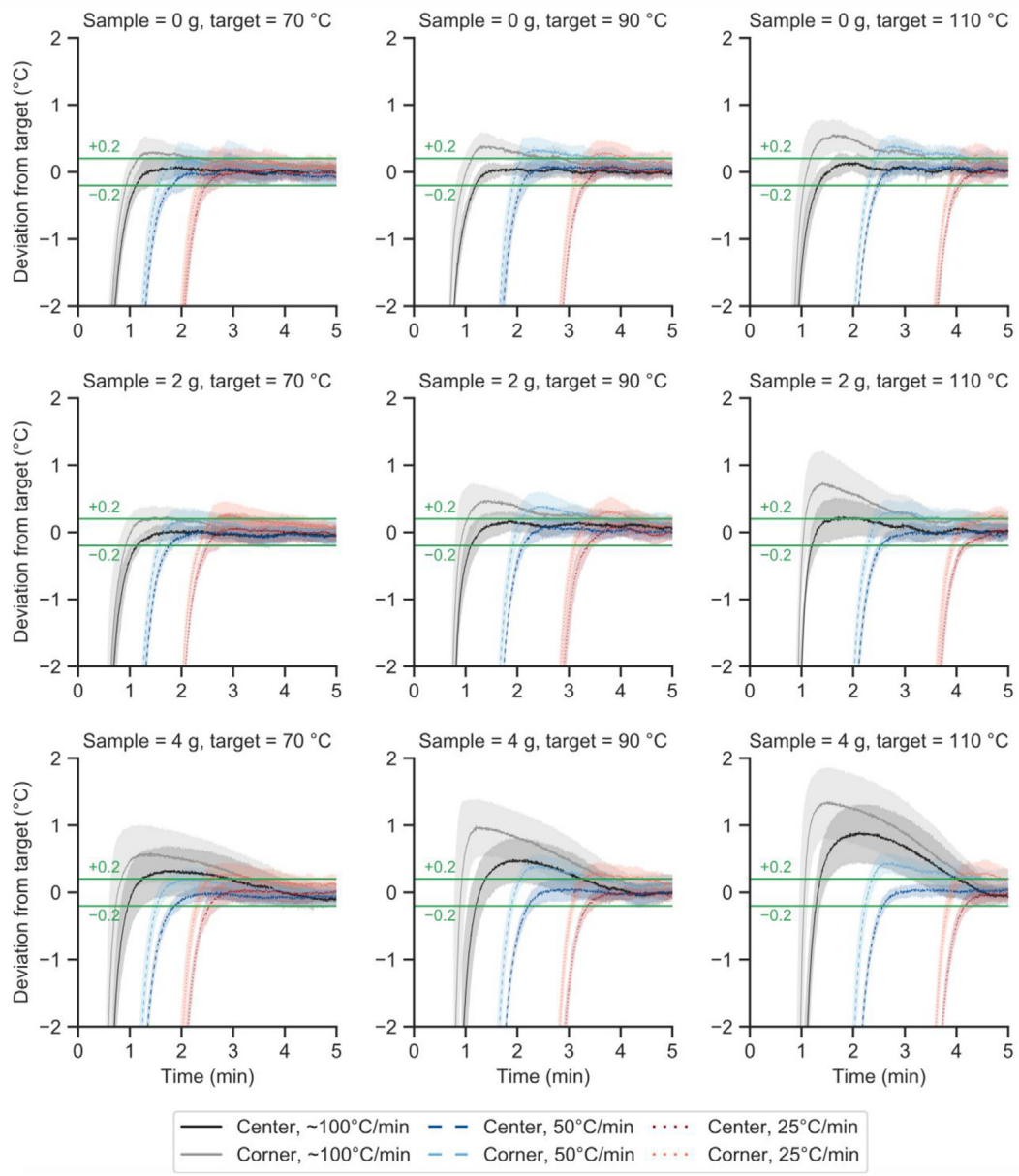

Fig. 9. Deviation of the center and corner temperatures of whole milk powder samples from the target temperature measured with various whole milk powder sample sizes (rows), target temperature (columns), and heating rates (line styles). Plotted lines are means of 12 TDT Sandwiches and are shrouded by one standard deviation. Green lines represent a ±0.2 °C boundary. (For interpretation of the references to color in this figure legend, the reader is referred to the web version of this article.)

Type-T 40 gage thermocouples (T1X-WBWX-40G-EX-0.25-PFXX-40-STWL, Evolution Sensors and Controls, West Deptford, NJ) were held in place with aluminum tape at the center and a corner of the sample pouches with one thermocouple per location. The pouches were then placed in the TDT Sandwich units. The thermocouples were connected to TDT Sandwiches that were not in use to acquire and record temperature readings at approximately 5 Hz.

The four characteristics for all operating parameter combinations are summarized in Table 7. In general, as the target temperature increased and/or heating rate decreased, t_{CUT} increased, which is expected due to larger heat requirement for a high target temperature and slower heating provided by a low heating rate. The standard deviation of t_{CUT} also appears to be the highest when the TDT Sandwich is operated at its maximum heating rate, with a maximum value of 6.8 s among all the operating conditions. At the CUT, the center of the sample was always colder than the corner, as evident by the negative $T_u^{t_{CUT}}$ values across all operating conditions, which agrees with the heat transfer model predictions from **Section 5.2**. In addition, $T_u^{t_{CUT}}$ appeared to increase if any one of the target temperatures, heating rates, or sample amounts increased. With a higher target temperature and heating rate, the system needs to provide more heat in a shorter time to bring the temperature of the heating pads up to the target. Since there is more sample mass at the center of the heating pad than the corner, the corner heats up faster and reaches a higher temperature. As the overall sample mass is increased, this discrepancy is aggravated. However, once the heating pads have reached the target temperature and enough time (1 min in this case) has been allowed for equilibration of the temperature of the sample, then the difference between the center and corner appears to be decreased, as evident by the smaller $T_u^{t_{SS}}$ values in comparison to $T_u^{t_{CUT}}$. At this point in time, $T_o^{t_{SS}}$ has also shrunk to almost zero, indicating that the heating pad temperature represents the temperature at the center of the sample at steady-state conditions. Therefore, it is not necessary to apply offsets to the target temperature when operating the TDT Sandwiches. The biggest exception to this is when the TDT Sandwiches were operated at maximum heating rate for samples with mass of 4 g. This observation arose because the sample had not yet achieved steady-state conditions at the 1 min mark, as will be discussed with Fig. 9.

The performance of the tested TDT Sandwich systems is visualized in Fig. 9 for all the operating conditions. As mentioned previously, the large value of $T_o^{t_{SS}}$ for 4 g samples heated at the maximum heating rate is caused by unsteady-state conditions; this can be seen in the lower three rows of Fig. 9 where the center and corner temperatures could take upwards of 4 min to settle at the target temperature. Therefore, operation of the TDT Sandwich at its maximum heating rate with a large amount of sample is not recommended. In addition, it is also apparent that the corner temperature tends to overshoot by more than 0.2 °C of the target temperature whenever the target temperature is 110 °C. These observations indicate that the parameters of the PI algorithm of the TDT Sandwich need to be adjusted for higher target temperatures; as of now, these parameters are constant values. Therefore, future versions of the system should introduce temperature dependency into the PI algorithm parameters (**Section 5.4**) to prevent overshoot at higher temperatures. In any case, the expected use cases for the TDT Sandwich would not require temperatures above 100 °C in order to avoid boiling of the food sample, therefore the system should be able to maintain the temperature of the sample within 0.2 °C of the target temperature. It is, however, advised to keep sample mass to minimum (2 g or less) to prevent the temperature overshoots as seen in the 4 g whole milk powder samples.

Declaration of Competing Interest

The authors declare that they have no known competing financial interests or personal relationships that could have appeared to influence the work reported in this paper.

Acknowledgements

This material is based upon work that is supported by the National Institute of Food and Agriculture, U.S. Department of Agriculture, under award number 2015-68003-23415. The first author would like to thank Kun Huang, Sierra Mendez, Raghavendra Singh, and Tushar Verma for their invaluable assistance during the process of manufacturing multiple TDT Sandwiches. The first author is also grateful to The Nebraska Innovation Studio for allowing use of their prototyping facilities.

References

[1] R.M. Syamaladevi, J. Tang, R. Villa-Rojas, S. Sablani, B. Carter, G. Campbell, Influence of water activity on thermal resistance of microorganisms in low-moisture foods: a review, Compr. Rev. Food Sci. Food Saf. 15 (2016) 353–370, https://doi.org/10.1111/1541-4337.12190.
[2] S. Condon, P. Lopez, R. Oria, F.J. Sala, Thermal death determination: design and evaluation of a thermoresistometer, J. Food Sci. 54 (1989) 451–457, https://doi.org/10.1111/j.1365-2621.1989.tb03104.x.
[3] S. Condón, M.J. Arrizubieta, F.J. Sala, Microbial heat resistance determinations by the multipoint system with the thermoresistometer TR-SC Improvement of this methodology, J. Microbiol. Methods. 18 (1993) 357–366. DOI:10.1016/0167-7012(93)90017-C.
[4] R. Conesa, S. Andreu, P. s. Fernández, A. Esnoz, A. Palop, Nonisothermal heat resistance determinations with the thermoresistometer Mastia, J. Appl. Microbiol. 107 (2009) 506–513. DOI:10.1111/j.1365-2672.2009.04236.x.
[5] M. Hassani, S. Condón, R. Pagán, Predicting microbial heat inactivation under nonisothermal treatments, J. Food Prot. 70 (2007) 1457–1467, https://doi.org/10.4315/0362-028X-70.6.1457.
[6] A. Palop, J. Raso, S. Condón, F.J. Sala, Heat resistance of Bacillus subtilis and Bacillus coagulans: effect of sporulation temperature in foods with various acidulants, J. Food Prot. 59 (1996) 487–492, https://doi.org/10.4315/0362-028X-59.5.487.

[7] F.J. Sala, P. Ibarz, A. Palop, J. Raso, S. Condon, Sporulation temperature and heat resistance of Bacillus subtilis at different pH values, J. Food Prot. 58 (1995) 239–243, https://doi.org/10.4315/0362-028X-58.3.239.
[8] A.M. Foster, L.P. Ketteringham, G.L. Purnell, A. Kondjoyan, M. Havet, J.A. Evans, New apparatus to provide repeatable surface temperature–time treatments on inoculated food samples, J. Food Eng. 76 (2006) 19–26, https://doi.org/10.1016/j.jfoodeng.2005.05.027.
[9] A.M. Foster, L.P. Ketteringham, M.J. Swain, A. Kondjoyan, M. Havet, O. Rouaud, J.A. Evans, Design and development of apparatus to provide repeatable surface temperature–time treatments on inoculated food samples, J. Food Eng. 76 (2006) 7–18, https://doi.org/10.1016/j.jfoodeng.2005.05.012.
[10] J.E. Gaze, A.R. Boyd, H.L. Shaw, Heat inactivation of Listeria monocytogenes Scott A on potato surfaces, J. Food Eng. 76 (2006) 27–31, https://doi.org/10.1016/j.jfoodeng.2005.05.035.
[11] R.J. Lewis, K. Robertson, H.M. Alloush, T. Dowman, V. Salisbury, Use of bioluminescence to evaluate the effects of rapid cooling on recovery of Salmonella enterica serovar Typhimurium DT104 after heat treatment, J. Food Eng. 76 (2006) 49–52, https://doi.org/10.1016/j.jfoodeng.2005.05.013.
[12] R.J. Lewis, A. Baldwin, T. O'Neill, H.A. Alloush, S.M. Nelson, T. Dowman, V. Salisbury, Use of Salmonella enterica serovar Typhimurium DT104 expressing lux genes to assess, in real time and in situ, heat inactivation and recovery on a range of contaminated food surfaces, J. Food Eng. 76 (2006) 41–48, https://doi.org/10.1016/j.jfoodeng.2005.05.023.
[13] M.S. McCann, J.J. Sheridan, D.A. McDowell, I.S. Blair, Effects of steam pasteurisation on Salmonella Typhimurium DT104 and Escherichia coli O157:H7 surface inoculated onto beef, pork and chicken, J. Food Eng. 76 (2006) 32–40, https://doi.org/10.1016/j.jfoodeng.2005.05.024.
[14] X. Kou, R. Li, L. Hou, Z. Huang, B. Ling, S. Wang, Performance of a heating block system designed for studying the heat resistance of bacteria in foods, Sci. Rep. 6 (2016) 30758, https://doi.org/10.1038/srep30758.
[15] L. Zhang, X. Kou, S. Zhang, T. Cheng, S. Wang, Effect of water activity and heating rate on Staphylococcus aureus heat resistance in walnut shells, Int. J. Food Microbiol. 266 (2018) 282–288, https://doi.org/10.1016/j.ijfoodmicro.2017.12.019.
[16] T. Cheng, R. Li, X. Kou, S. Wang, Influence of controlled atmosphere on thermal inactivation of Escherichia coli ATCC 25922 in almond powder, Food Microbiol. 64 (2017) 186–194, https://doi.org/10.1016/j.fm.2017.01.007.
[17] S. Zhang, L. Zhang, R. Lan, X. Zhou, X. Kou, S. Wang, Thermal inactivation of Aspergillus flavus in peanut kernels as influenced by temperature, water activity and heating rate, Food Microbiol. 76 (2018) 237–244, https://doi.org/10.1016/j.fm.2018.05.015.
[18] T. Cheng, S. Wang, Influence of storage temperature/time and atmosphere on survival and thermal inactivation of Escherichia coli ATCC 25922 inoculated to almond powder, Food Control. 86 (2018) 350–358, https://doi.org/10.1016/j.foodcont.2017.11.029.
[19] M. Al-Holy, Z. Quinde, D. Guan, J. Tang, B. Rasco, Thermal Inactivation of Listeria innocua in Salmon (Oncorhynchus keta) caviar using conventional glass and novel aluminum thermal-death-time tubes, J. Food Prot. 67 (2004) 383–386, https://doi.org/10.4315/0362-028X-67.2.383.
[20] H.-J. Chung, S. Wang, J. Tang, Influence of heat transfer with tube methods on measured thermal inactivation parameters for Escherichia coli, J. Food Prot. 70 (2007) 851–859, https://doi.org/10.4315/0362-028X-70.4.851.
[21] T.L. Bergman, A.S. Lavine, F.P. Incropera, D.P. DeWitt, Fundamentals of Heat and Mass Transfer, seventh ed., Wiley, Hoboken, NJ, 2011.
[22] B.G. Liptak, ed., Instrument Engineers' Handbook, Volume Two: Process Control and Optimization, CRC Press, 2018.
[23] Y. Kikoku, N. Tagashira, H. Nakano, Heat resistance of fungi isolated from frozen blueberries, J. Food Prot. 71 (2008) 2030–2035, https://doi.org/10.4315/0362-028X-71.10.2030.
[24] V. Tournas, R.W. Traxler, Heat resistance of a Neosartorya fischeri strain isolated from pineapple juice frozen concentrate, J. Food Prot. 57 (1994) 814–816, https://doi.org/10.4315/0362-028X-57.9.814.
[25] V. Carlier, J.C. Augustin, J. Rozier, Heat Resistance of Listeria monocytogenes (Phagovar 2389/2425/3274/2671/47/108/340): D- and z-Values in Ham, J. Food Prot. 59 (1996) 588–591, https://doi.org/10.4315/0362-028X-59.6.588.
[26] V. Mulak, R. Tailliez, P. Eb, P. Becel, Heat resistance of bacteria isolated from preparations based on seafood products, J. Food Prot. 58 (1995) 49–53, https://doi.org/10.4315/0362-028X-58.1.49.
[27] J.D. Schuman, B.W. Sheldon, P.M. Foegeding, Thermal resistance of aeromonas hydrophila in liquid whole egg, J. Food Prot. 60 (1997) 231–236, https://doi.org/10.4315/0362-028X-60.3.231.
[28] A.E.H. Shearer, A.S. Mazzotta, R. Chuyate, D.E. Gombas, Heat resistance of juice spoilage microorganisms, J. Food Prot. 65 (2002) 1271–1275, https://doi.org/10.4315/0362-028X-65.8.1271.
[29] D.F. Splittstoesser, M.R. Mclellan, J.J. Churey, Heat resistance of Escherichia coli O157:H7 in apple juice, J. Food Prot. 59 (1996) 226–229, https://doi.org/10.4315/0362-028X-59.3.226.
[30] T.C. Jackson, M.D. Hardin, G.R. Acuff, Heat resistance of Escherichia coli O157:H7 in a nutrient medium and in ground beef patties as influenced by storage and holding temperatures, J. Food Prot. 59 (1996) 230–237, https://doi.org/10.4315/0362-028X-59.3.230.
[31] M. Peña-Meléndez, J.J. Perry, A.E. Yousef, Changes in thermal resistance of three Salmonella Serovars in response to osmotic shock and adaptation at water activities reduced by different humectants, J. Food Prot. 77 (2014) 914–918, https://doi.org/10.4315/0362-028X.JFP-13-201.
[32] E. Enache, A. Kataoka, D.G. Black, L. Weddig, M. Hayman, K. Bjornsdottir-Butler, Heat resistance of histamine-producing bacteria in irradiated tuna loins, J. Food Prot. 76 (2013) 1608–1614, https://doi.org/10.4315/0362-028X.JFP-12-467.
[33] I.M. Hildebrandt, B.P. Marks, V.K. Juneja, M. Osoria, N.O. Hall, E.T. Ryser, Cross-laboratory comparative study of the impact of experimental and regression methodologies on salmonella thermal inactivation parameters in ground beef, J. Food Prot. 79 (2016) 1097–1106, https://doi.org/10.4315/0362-028X.JFP-15-496.
[34] D. Karyotis, P.N. Skandamis, V.K. Juneja, Thermal inactivation of Listeria monocytogenes and Salmonella spp. in sous-vide processed marinated chicken breast, Food Res. Int. 100 (2017) 894–898, https://doi.org/10.1016/j.foodres.2017.07.078.
[35] L. Li, J. Cepeda, J. Subbiah, G. Froning, V.K. Juneja, H. Thippareddi, Dynamic predictive model for growth of Salmonella spp. in scrambled egg mix, Food Microbiol. 64 (2017) 39–46, https://doi.org/10.1016/j.fm.2016.12.007.
[36] A.S. Mazzotta, Heat resistance of listeria monocytogenes in vegetables: evaluation of blanching processes, J. Food Prot. 64 (2001) 385–387, https://doi.org/10.4315/0362-028X-64.3.385.
[37] A.S. Mazzotta, Thermal inactivation of stationary-phase and salt-adapted listeria monocytogenes during postprocess pasteurization of surimi-based imitation crab meat, J. Food Prot. 64 (2001) 483–485, https://doi.org/10.4315/0362-028X-64.4.483.
[38] M. Redondo-Solano, D.E. Burson, H. Thippareddi, Thermal resistance of clostridium difficile spores in peptone water and pork meat, J. Food Prot. 79 (2016) 1468–1474, https://doi.org/10.4315/0362-028X.JFP-15-579.
[39] H.-J. Chung, S.L. Birla, J. Tang, Performance evaluation of aluminum test cell designed for determining the heat resistance of bacterial spores in foods, LWT - Food Sci. Technol. 41 (2008) 1351–1359, https://doi.org/10.1016/j.lwt.2007.08.024.
[40] I.M. Hildebrandt, B.P. Marks, E.T. Ryser, R. Villa-Rojas, J. Tang, F.J. Garces-Vega, S.E. Buchholz, Effects of inoculation procedures on variability and repeatability of salmonella thermal resistance in wheat flour, J. Food Prot. 79 (2016) 1833–1839, https://doi.org/10.4315/0362-028X.JFP-16-057.
[41] T. Jin, H. Zhang, G. Boyd, J. Tang, Thermal resistance of Salmonella enteritidis and Escherichia coli K12 in liquid egg determined by thermal-death-time disks, J. Food Eng. 84 (2008) 608–614, https://doi.org/10.1016/j.jfoodeng.2007.06.026.
[42] D.F. Smith, I.M. Hildebrandt, K.E. Casulli, K.D. Dolan, B.P. Marks, Modeling the effect of temperature and water activity on the thermal resistance of Salmonella Enteritidis PT 30 in wheat flour, J. Food Prot. 79 (2016) 2058–2065, https://doi.org/10.4315/0362-028X.JFP-16-155.
[43] D.F. Smith, B.P. Marks, Effect of rapid product desiccation or hydration on thermal resistance of salmonella enterica serovar enteritidis PT 30 in wheat flour, J. Food Prot. 78 (2015) 281–286, https://doi.org/10.4315/0362-028X.JFP-14-403.
[44] J.J. Perry, A.E. Yousef, Factors affecting thermal resistance of salmonella enterica serovar enteritidis ODA 99–30581-13 in shell egg contents and use of heat-ozone combinations for egg pasteurization, J. Food Prot. 76 (2013) 213–219, https://doi.org/10.4315/0362-028X.JFP-12-324.